



ARL-TR-8791 • SEP 2019



Characterization and Modeling of the In-Plane Shear Deformation in Ultra-High Molecular Weight Polyethylene (UHMWPE) Composites

by Michael Yeager, Julia Cline, Kari White, Travis Bogetti, and James Sherwood

Approved for public release; distribution is unlimited.

NOTICES

Disclaimers

The findings in this report are not to be construed as an official Department of the Army position unless so designated by other authorized documents.

Citation of manufacturer's or trade names does not constitute an official endorsement or approval of the use thereof.

Destroy this report when it is no longer needed. Do not return it to the originator.



Characterization and Modeling of the In-Plane Shear Deformation in Ultra-High Molecular Weight Polyethylene (UHMWPE) Composites

Michael Yeager, Julia Cline, and Travis Bogetti
Weapons and Materials Research Directorate, CCDC Army Research Laboratory

Kari White and James Sherwood
University of Massachusetts Lowell

REPORT DOCUMENTATION PAGE

*Form Approved
OMB No. 0704-0188*

Public reporting burden for this collection of information is estimated to average 1 hour per response, including the time for reviewing instructions, searching existing data sources, gathering and maintaining the data needed, and completing and reviewing the collection information. Send comments regarding this burden estimate or any other aspect of this collection of information, including suggestions for reducing the burden, to Department of Defense, Washington Headquarters Services, Directorate for Information Operations and Reports (0704-0188), 1215 Jefferson Davis Highway, Suite 1204, Arlington, VA 22202-4302. Respondents should be aware that notwithstanding any other provision of law, no person shall be subject to any penalty for failing to comply with a collection of information if it does not display a currently valid OMB control number.

PLEASE DO NOT RETURN YOUR FORM TO THE ABOVE ADDRESS.

1. REPORT DATE (DD-MM-YYYY) September 2019		2. REPORT TYPE Technical Report		3. DATES COVERED (From - To) 25 January 2018–20 August 2019	
4. TITLE AND SUBTITLE Characterization and Modeling of the In-Plane Shear Deformation in Ultra-High Molecular Weight Polyethylene (UHMWPE) Composites				5a. CONTRACT NUMBER	
				5b. GRANT NUMBER	
				5c. PROGRAM ELEMENT NUMBER	
6. AUTHOR(S) Michael Yeager, Julia Cline, Kari White, Travis Bogetti, and James Sherwood				5d. PROJECT NUMBER	
				5e. TASK NUMBER	
				5f. WORK UNIT NUMBER	
7. PERFORMING ORGANIZATION NAME(S) AND ADDRESS(ES) CCDC Army Research Laboratory ATTN: FCDD-RLW-MA Aberdeen Proving Ground, MD 21005				8. PERFORMING ORGANIZATION REPORT NUMBER ARL-TR-8791	
9. SPONSORING/MONITORING AGENCY NAME(S) AND ADDRESS(ES)				10. SPONSOR/MONITOR'S ACRONYM(S)	
				11. SPONSOR/MONITOR'S REPORT NUMBER(S)	
12. DISTRIBUTION/AVAILABILITY STATEMENT Approved for public release; distribution is unlimited.					
13. SUPPLEMENTARY NOTES ORCID ID: Cline, 0000-0003-1994-3247; Yeager, 0000-0001-8528-1072					
14. ABSTRACT Ultra-high molecular weight polyethylene (UHMWPE) composites are employed in wide array of ballistic protective applications, where there is a close relationship between the as-manufactured component quality and performance. Thermoforming is an efficient way to produce a large volume of complex curvature thermoplastic parts for ballistic protective systems, such as helmets. During the thermoforming process, commercially available thin sheets of UHMWPE material are stacked loosely before undergoing a preforming process at elevated temperature. The near-net shape “preforms” subsequently undergo high-pressure consolidation. In the preforming process, the individual sheets of UHMWPE composite are subjected to large amounts of in-plane shear deformation. Accurate characterization of the in-plane shear response is critical in developing reliable predictive models capable of guiding process cycle design. This work establishes a methodology for characterizing the in-plane shear response of UHMWPE composites using the bias-extension test method. An LS-DYNA finite-element model, capable of simulating the in-plane shear behavior of the UHMWPE composite, is presented and verified by predicting the results from the bias-extension test. The LS-DYNA model and characterization methodology are further validated through correlation of predicted results with experimental observations using the picture frame test.					
15. SUBJECT TERMS UHMWPE composites, material characterization, DIC analysis, finite element modeling, in-plane shear constitutive response					
16. SECURITY CLASSIFICATION OF:			17. LIMITATION OF ABSTRACT UU	18. NUMBER OF PAGES 27	19a. NAME OF RESPONSIBLE PERSON Michael Yeager
a. REPORT Unclassified	b. ABSTRACT Unclassified	c. THIS PAGE Unclassified			19b. TELEPHONE NUMBER (Include area code) (410) 306-0681

Contents

List of Figures	iv
Acknowledgments	v
1. Introduction	1
1.1 Motivation	1
1.2 Background	2
2. Methodology	4
2.1 Materials	4
2.2 Bias-Extension Experimental Setup	4
2.3 Picture Frame Experimental Setup	5
2.4 Bias-Extension Data Analysis	6
2.5 Numerical Model Setup	10
3. Results and Discussion	11
3.1 Bias-Extension Test	11
3.2 Bias-Extension Simulation	12
3.3 Picture Frame Model Predictions and Experimental Results	14
4. Conclusions	16
5. References	18
Distribution List	20

List of Figures

Fig. 1	Preforming of UHMWPE sheets into a complex curvature part	1
Fig. 2	Pure shear region in specimens with aspect ratios of a) 3:1 and b) 7:1	3
Fig. 3	Experimental setup for the bias-extension test	5
Fig. 4	Experimental setup for the picture frame test: a) cruciform specimen and b) frame in initial and sheared positions	6
Fig. 5	Bias-extension specimen gage length with pure shear region and necessary geometry labeled	7
Fig. 6	Free body diagram of pure shear region bounds.....	8
Fig. 7	Boundary conditions for a) bias-extension and b) picture frame models	11
Fig. 8	Shear stress–strain response for fiber-based (HB210) and film-based (Tensylon) systems	12
Fig. 9	Experimentally derived shear response and corresponding trilinear fit for HB210	13
Fig. 10	Representative shear strain prediction for HB210 after 20 mm of crosshead displacement.....	13
Fig. 11	Bias-extension simulation and experimental results for fiber-based (HB210) and film-based (Tensylon) systems	14
Fig. 12	Picture frame test simulation results, using characterized in-plane shear response, compared to experimental results	15
Fig. 13	Shear strain distribution in the picture frame model for HB210 at 40-mm crosshead displacement	16

Acknowledgments

The authors acknowledge Jim Wolbert, Mike Neblett, and Freddie Racine, all of the US Army Combat Capabilities Development Command Army Research Laboratory (CCDC ARL), for cutting the bias-extension specimens used in this work. Additionally, the work of Dr Tim Walter, David Gray, and Paul Moy in developing the test set up is gratefully acknowledged.

This research was supported in part by ARL under Cooperative Agreement Number W911NF-18-2-0033. The views and conclusions contained in this document are those of the authors and should not be interpreted as representing the official policies, either expressed or implied, of ARL or the US Government.

1. Introduction

1.1 Motivation

Ultra-high molecular weight polyethylene (UHMWPE) composite is a common component of helmets for ballistic protection due to its high strength and light weight.¹ Individual sheets of UHMWPE are typically manufactured as flat sheets with aligned fibers or films embedded in a thermoplastic polymer matrix. Developing process models capable of accurately predicting the manufacture of parts with complex compound curvatures from flat sheets is challenging.² Due to the complexities and export control restrictions associated with helmet geometries, most readily available literature simplifies the problem to a hemispherical geometry.^{1,3,4}

A multistage process is used to manufacture compound curvature parts for ballistic protection. The first step is to preform the flat sheets into a near final shape or geometry. The preformed stack of UHMWPE sheets then undergo high pressure and temperature consolidation between matched metal tooling.^{1,3,4}

The preforming process, shown in Fig. 1, involves a punch operation that deforms the UHMWPE sheets as they pass through a die plate.¹ A binder ring provides pressure on the stack of flat sheets that, in turn, induces in-plane tension to mitigate wrinkling. The out-of-plane constraint from the binder, along with in-plane loading of the sheet via friction at the sheet-tooling interfaces, causes shear deformation within the sheets during preforming. The main shear deformation mechanism is attributed to fiber rotation.⁵ Shear deformation gradients lead to thickness variations in the preform, which in turn lead to undesirable pressure gradients in the consolidation phase.¹ Nonuniform pressure gradients can result in a situation where the preform is exposed to excessive pressures in certain regions and lacking sufficient pressure for proper consolidation in others. As previous work has demonstrated the importance of consolidation pressure on the mechanical properties and ballistic performance of UHMWPE composites,^{6,7} the situation of nonuniform pressure inherently compromises the quality, reproducibility, and performance of the as-manufactured part.

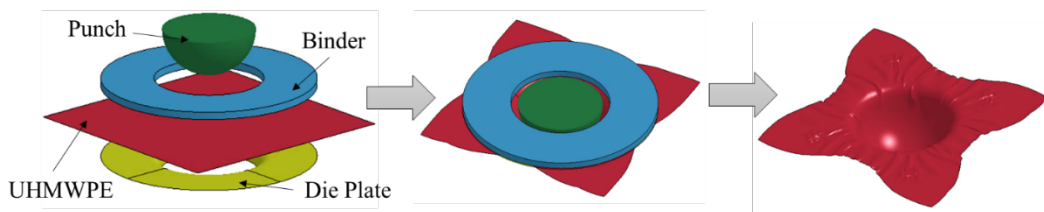


Fig. 1 Preforming of UHMWPE sheets into a complex curvature part

1.2 Background

The picture frame and bias-extension tests are commonly used to characterize the shear behavior of materials for forming applications. The shear behavior of “fiber-based” UHMWPE systems has successfully been characterized using the picture frame test.⁸ Thin “film-based” UHMWPE systems have been found to be much more problematic, as they wrinkle and tear during the picture frame test.⁹ The presence of deformation mechanisms other than pure shear in the gage section of the film-based specimens prohibits the use of existing picture frame characterization methodologies for UHMWPE composites⁸ and textiles.¹⁰

The bias-extension test has been used to characterize woven textile systems, but has not frequently been used to obtain shear constitutive relationships for sheets of UHMWPE.¹¹ The experiment consists of in-plane tension being applied to a specimen with reinforcement oriented at a $\pm 45^\circ$ angle, resulting in shear loading within the gage section. There is a large volume of published work on the bias-extension test, which is summarized in a recent review paper.¹¹ Most of the shear characterization work in the literature is focused on woven textiles,¹⁰ which are fundamentally different than UHMWPE cross-ply systems. The major difference is that woven textiles exhibit a shear locking phenomenon in which the shear stiffness greatly increases after a critical shear angle due to the pin joint no longer permitting tow rotation.¹² The unidirectional, nonwoven nature of the UHMWPE reinforcement eliminates the traditional shear locking phenomenon because the warp and weft fibers are not in the same plane.

Results obtained for woven textile specimens can be adversely influenced by edge effects and tow width. A benchmark study found that the length-to-width aspect ratio of a typical woven textile specimen should be between 2:1 and 3:1.¹⁰ The unidirectional nature of UHMWPE systems allows for the use of narrower specimens (2.54 cm [1 inch]) with large aspect ratios (7:1) without edge effects or handling issues. The pure shear region in long, thin specimens is much larger (normalized by total specimen area) than with typical geometries discussed previously (Fig. 2). The effects of the regions of combined shear and tension need to be included in the 3:1 specimen but are small enough to be neglected in the 7:1 specimen.

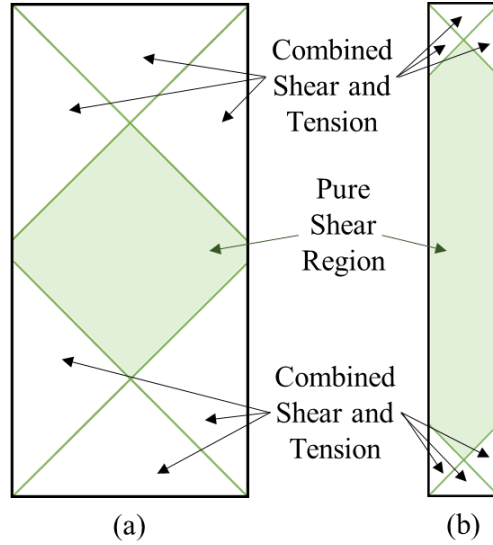


Fig. 2 Pure shear region in specimens with aspect ratios of a) 3:1 and b) 7:1

The shear strain in the narrow, long pure shear region can be analyzed with digital image correlation (DIC). Narrower width specimens enable higher resolution of strain field imaging while still capturing the entire width (which permits confirmation that the strain field is uniform throughout the width) as opposed to having a gradient close to the edges. DIC analysis provides more accurate shear strain values than an analytically based analysis because it removes geometric and uniform strain field assumptions.

ASTM D3518/3518M-13 describes a methodology for converting axial load output to shear stress through¹³:

$$\tau = \frac{P}{2A}, \quad (1)$$

where P is the measured axial force and A is the cross-sectional area, calculated by multiplying the original specimen width and thickness. The ASTM method assumes a constant 90° angle between fibers, which is why it is not valid for large engineering shear strains.¹³ In preforming, shear strains typically exceed the applicable range of the ASTM standard, often reaching upward 50° of engineering shear strain.¹

This report shows how relaxing the angle constraint in the ASTM analysis allows the computation of shear stress during bias-extension tests beyond the 5% axial strain limit associated with Eq. 1 (which from geometry correlates to about 5° [0.087 radians] of shear deformation). A methodology to determine the in-plane shear constitutive response of both fiber- and film-based UHMWPE systems is

presented and evaluated. The shear strain is calculated using DIC, and the shear stress is computed using the tensile load measured by the Instron. The shear stress–strain curve is input into numerical models of the bias-extension and picture frame tests. Predictions from the model are compared to bias-extension and picture frame experimental results for a fiber-based UHMWPE system to validate the methodology. They also provide insight into the shear-strain distribution throughout the specimens.

2. Methodology

2.1 Materials

DSM Dyneema HB210¹⁴ and DuPont Tensylon HSBD 30A¹⁵ were selected as the UHMWPE fiber- and film-based material, respectively, for this work. A single sheet of the HB210 material system consists of four unidirectional plies (polyethylene fibers embedded in a polyethylene matrix) oriented in a $[0/90]_2$ configuration. In contrast, a single sheet of Tensylon 30A contains two perpendicular plies of a highly oriented solid-state extruded tape, oriented in a $[0/90]$ configuration.

2.2 Bias-Extension Experimental Setup

Dyneema HB210 and Tensylon 30A sheets are waterjet cut into specimens measuring 30.48 cm long by 2.54 cm wide with fiber orientations of $\pm 45^\circ$ relative to the length of the specimen. Specimens are dried after waterjet cutting to ensure moisture absorption would not influence mechanical properties. To enable DIC measurement of the deformation field, a black and white random speckle pattern is applied to the specimen surface using spray paint.

Specimens are loaded in tension using an Instron 1125 5500R electromechanical test frame with a 5-kN load cell. Adequate gripping is achieved using wedge action grips with lightly serrated grip faces. The off-axis fibers significantly reduce grip slip typically encountered when testing UHMWPE composites. Tests are conducted at a rate of 12.7 mm/min until delamination failure.

For each material configuration, five specimens are tested. Figure 3 shows the experimental setup, including stereovision DIC camera setup. Two 2.3-MPixel Point Grey Cameras with Nikon 55-mm lenses are used to capture images of the deforming surface, as shown in Fig. 3. The cameras are focused on the center section of the specimen. Correlated Solutions' Vic Snap and Vic 3D software

(<http://www.correlatedsolutions.com>) are used to capture and analyze images, respectively, at 1 frame per second. Applied load is recorded for each image.

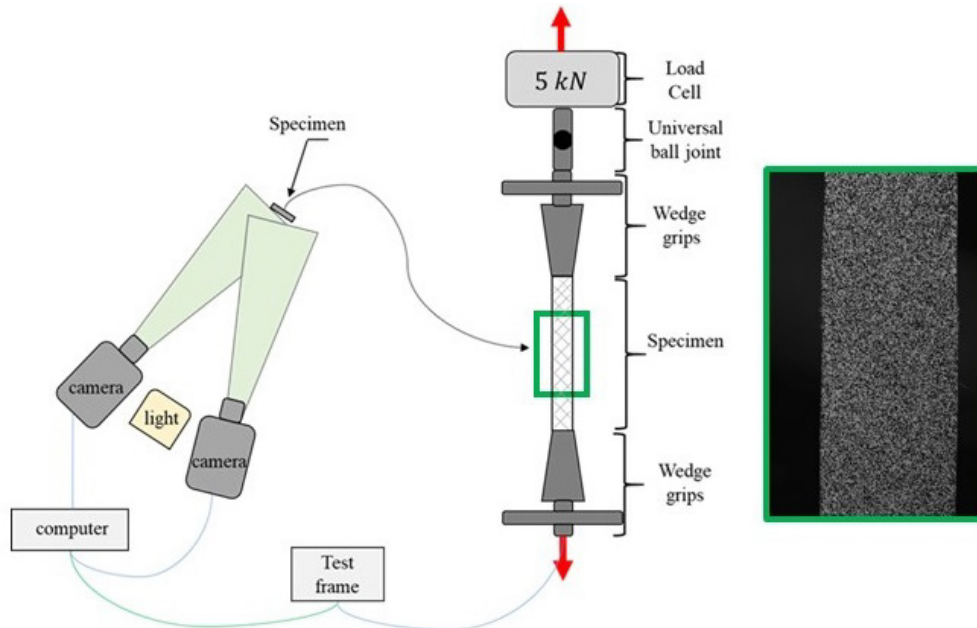


Fig. 3 Experimental setup for the bias-extension test

2.3 Picture Frame Experimental Setup

Only Dyneema HB210 picture frame data are presented due to challenges in testing the Tensylon 30A. Dyneema HB210 is cut with an electric rotary cutter into cruciform-shaped specimens with 127-mm sides in the central region aligned with the fiber direction and arms extended to fit into the 216-mm side length of the frame (Fig. 4a). The specimen is mounted in a picture frame testing fixture that is hinged at the four corners, and a displacement is applied to the top of the testing rig (Fig. 4b). The top corner displacement induces a state of pure shear to the central region of the specimen.

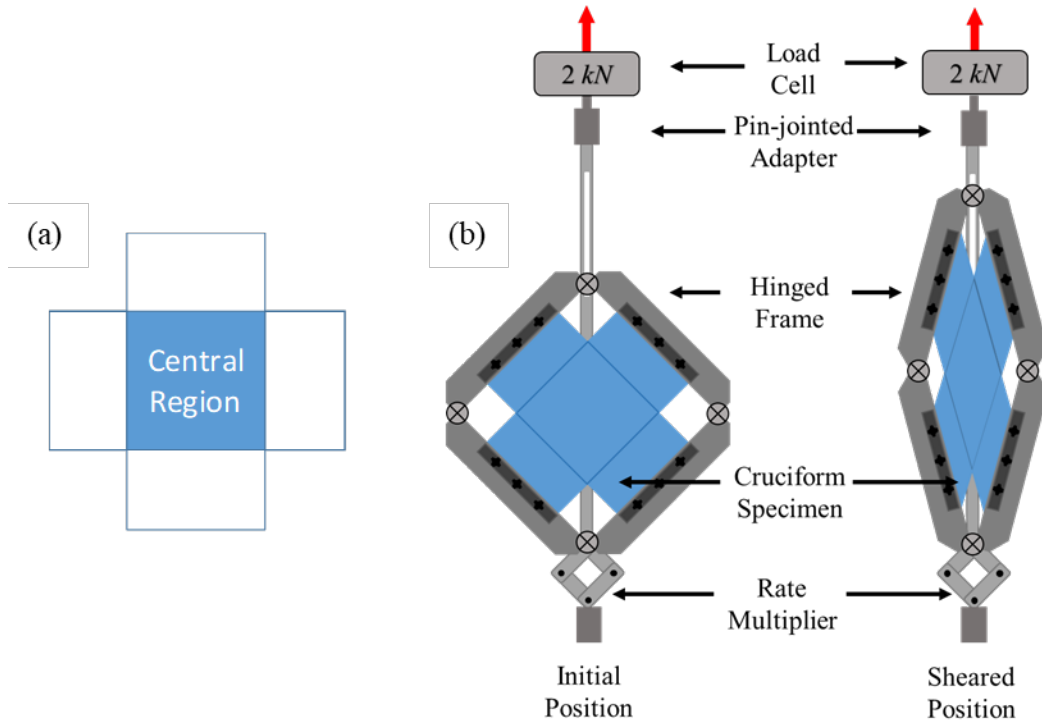


Fig. 4 Experimental setup for the picture frame test: a) cruciform specimen and b) frame in initial and sheared positions

The test rig (specially designed and manufactured at the University of Massachusetts Lowell) with the mounted specimen is installed into an Instron 4464 universal testing machine with 2-kN load cell. The crosshead rate for the shear frame is 2 mm/s, which corresponds to a rate of 8.5 mm/s on the specimen, made possible by the multiplier built into the shear frame. The total displacement of the crosshead is 25.4 mm, corresponding to 108 mm of displacement on the top corner of the specimen. The shear strain in the specimen can be calculated from the geometric relationship between the top displacement and the frame arms. Load and displacement data are recorded via the Instron software.

2.4 Bias-Extension Data Analysis

Previous research has shown that both Dyneema HB210 and Tensylon 30A undergo finite deformations in this test configuration,⁵ just as the material will when preformed. Fiber rotation (or fiber scissoring) is a well-known deformation mechanism for UHMWPE materials that needs to be included in preforming models.

The analysis method outlined by Cline et al.⁵ is used to calculate the fiber rotation angles for both material systems. The initial configuration of the fibers can be represented as two orthogonal vectors, \vec{A} and \vec{B} , that are oriented at $\pm 45^\circ$ from the

loading direction. As load is applied and deformation occurs, the fibers rotate to a new position defined by vectors \vec{a} and \vec{b} , oriented at $\pm\theta^\circ$ from the vertical axis, where $\theta < 45^\circ$.

The relationship between the deformed and undeformed vectors is defined as the deformation tensor, \mathbf{F} , given by

$$\mathbf{F} = \begin{bmatrix} \lambda & 0 & 0 \\ 0 & \alpha & 0 \\ 0 & 0 & \beta \end{bmatrix}, \quad (2)$$

where it is assumed there are no shear components to the deformation in this case. The diagonal matrix elements, λ, α, β , are the stretches in the 1, 2, 3 directions, respectively. The 1, 2, 3 directions define the axial, transverse, and through-thickness ply coordinate system directions as shown in Fig. 5 (with the through thickness direction being out of the page). Deformation in the through thickness direction is not considered in this analysis. The stretches can be calculated from the Lagrangian strains calculated using the DIC software as a function of load step using the following relationship for the Green-Lagrange strain tensor:

$$\mathbf{E} = 0.5 * (\mathbf{C} - \mathbf{I}) = 0.5 * (\mathbf{F}^T \mathbf{F} - \mathbf{I}). \quad (3)$$

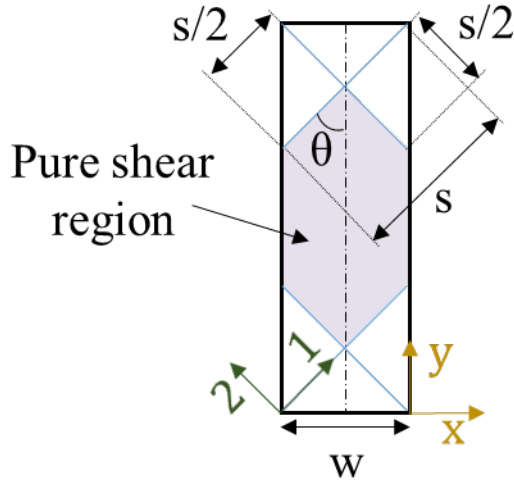


Fig. 5 Bias-extension specimen gage length with pure shear region and necessary geometry labeled

It follows that $\vec{a} = \mathbf{F}\vec{A}$ and $\vec{b} = \mathbf{F}\vec{B}$. By computing the angle between vectors \vec{a} and \vec{b} , the rotated fiber angle can be calculated as a function of the stretches, $\lambda(E_1)$ and $\alpha(E_2)$.

$$\theta = \frac{1}{2} \cos^{-1} \left(\frac{\vec{a} \cdot \vec{b}}{\|\vec{a}\| \cdot \|\vec{b}\|} \right) = \frac{1}{2} \cos^{-1} \left(\frac{(\lambda(E_1)^2 - \alpha(E_2)^2)}{(\lambda(E_1)^2 + \alpha(E_2)^2)} \right). \quad (4)$$

During the bias-extension test, a large pure-shear region will develop in areas that do not contain any fibers involved in the boundary constraint created by the machine grips, as shown in Fig. 5. A force balance in the pure-shear region yields the following relationship between the fiber rotation angle (θ in Fig. 5), shear force (F_s), and axial force (F_y) measured by the Instron and illustrated in Fig. 6:

$$F_y = F_s \cos\theta + F_s \cos\theta. \quad (5)$$

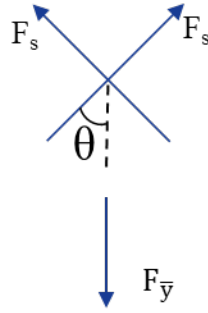


Fig. 6 Free body diagram of pure shear region bounds

The force component normal to the shear force is not included in the force balance because the section is in pure shear, making the normal component zero. Accordingly, Eq. 5 can be rearranged to

$$F_s = \frac{F_y}{2 \cos\theta}. \quad (6)$$

The corresponding shear stress, defined as force per unit area, is given as

$$\tau_{12} = \frac{F_y}{2 s t \cos\theta}, \quad (7)$$

where τ is the in-plane (12-direction) shear, s is the length of the pure-shear region top boundary, and t is the thickness of the specimen.

UHMWPE fiber- and film-based systems have been shown to rotate but not extend in the fiber direction during bias-extension experiments.⁵ The systems are also assumed not to extend in the transverse direction because the bond between plies ensures that transverse deformation requires fiber extension in neighboring plies.

Delamination would load the plies in the transverse direction but subsequently cause material failure and an end to the test as the plies are weak in the transverse direction. Knowing that extension in both the fiber and transverse directions of each ply are negligible, the Pythagorean theorem allows s to be written as

$$s = \sqrt{2} w. \quad (8)$$

The lack of fiber extension ensures s will be constant, allowing the relationship in Eq. 8 (based on the initial width) to be carried throughout the analysis. If fiber extension is not negligible, this assumption becomes invalid and instead s should be found experimentally (e.g., computed with DIC) and used in Eq. 7.

The thickness of the specimen changes as a result of shear deformation and would be very difficult to measure at each time step during the test, particularly with the edges frayed a small amount during material cutting. Previous work has shown that the volume is conserved during the shearing of UHMWPE systems, allowing the thickness (t) at a given deformation state to be written in terms of the original specimen thickness and the fiber orientation angle¹:

$$t = \frac{t_{\text{undeformed}}}{\sin(2\theta)}. \quad (9)$$

Here, $t_{\text{undeformed}}$ is the thickness of the specimen prior to testing. The relationship between fiber rotation angle (θ) (computed through DIC) and shear strain (γ_{12}), is

$$\theta = \frac{\pi}{4} - \frac{\gamma_{12}}{2}. \quad (10)$$

Substituting Eqs. 8–10 into Eq. 7 yields the shear stress as a function of the force measured with the Instron and the shear angle from DIC:

$$\tau_{12} = \frac{F_y \sin\left(\frac{\pi}{2} - \gamma_{12}\right)}{2\sqrt{2} w t_{\text{undeformed}} \cos\left(\frac{\pi}{4} - \frac{\gamma_{12}}{2}\right)}. \quad (11)$$

Using trigonometric relationships (double-angle formula, etc.) and algebra, Eq. 11 can be rearranged as follows:

$$\tau_{12} = \frac{F_y \left[\cos\left(\frac{\gamma_{12}}{2}\right) - \sin\left(\frac{\gamma_{12}}{2}\right) \right]}{2 w t_{\text{undeformed}}}. \quad (12)$$

Equation 12, along with the DIC shear strain values, can now be used to characterize the shear stress–strain constitutive response for UHMWPE materials,

for large shear strains that are well beyond the 5% limit inherent in the ASTM D3518¹³ data reduction method.

2.5 Numerical Model Setup

Finite-element-based models are developed in LS-DYNA to describe the UHMWPE sheet deformation during both the bias-extension and picture frame tests. The explicit dynamics models include mass scaling to reduce simulation time and use a fabric material model (MAT214). MAT214 requires the input of elastic moduli in the axial and transverse directions of the sheet (both the same for this work), as well as a trilinear shear modulus curve.¹⁶ The directions of the fibers within the sheets are updated and tracked at each time step to account for fiber rotation. A user input option in MAT214 is used that allows for sheet orientation to be independent of meshing. Fully integrated (LS-DYNA, Type 16) and Belytschko-Tsay (LS-DYNA, Type 2) shell elements¹⁷ are both suitable for this work, although the Belytschko-Tsay elements were favored for their computational efficiency.

The bias-extension model, shown in Fig. 7a, includes the 177.8- × 25.4-mm gage section of a UHMWPE specimen. Nodes along the top boundary are prescribed a uniform displacement rate in the axial loading direction while those on the bottom are fixed. Rate-dependent properties are not included in this model because the test is being performed at a quasi-static rate (12.7 mm/min). Accordingly, model predictions are independent of the displacement rate of the top nodes. The fiber orientations within the plies are assumed to be $\pm 45^\circ$ from the axial load direction (diagonal to the elements in the model).

The picture frame model, with dimensions to match the experimental setup, includes the UHMWPE specimen and the four-part frame, as depicted in Fig. 7b. The hinge at the top of the frame has a prescribed displacement, while the bottom hinge has a fixed boundary condition. The frame consists of four parts (sides), each with elastic material properties (MAT_ELASTIC). The frame sides comprise shells that are extremely thick (150 times the UHMWPE thickness) and have a high elastic modulus (10 times that of the UHMWPE) to ensure they will behave as rigid bodies during the simulation. This combination is to ensure the boundaries of the UHMWPE in the model experience a negligible amount of deformation, making them consistent with those of the experiment.

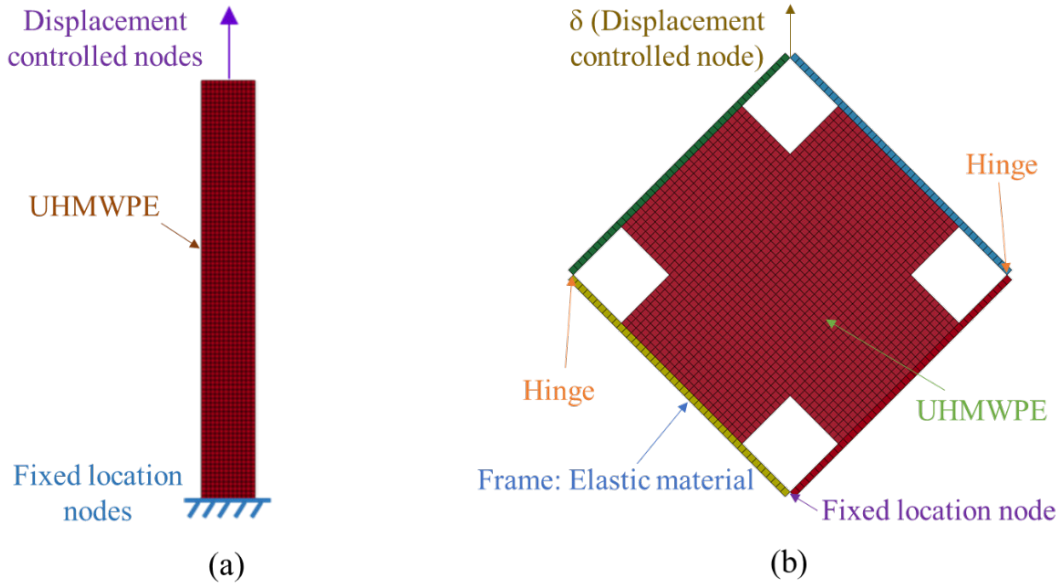


Fig. 7 Boundary conditions for a) bias-extension and b) picture frame models

3. Results and Discussion

The bias-extension test is used to characterize the in-plane shear response of the UHMWPE material. Predicting the picture frame experimental results using input properties from the bias-extension test will serve as validation of both the model and the shear characterization methodology.

3.1 Bias-Extension Test

DIC images for each specimen test are imported into VIC3D correlation software.¹⁶ The incremental correlation option is selected within the software to ensure that large deformation is captured accurately. Incremental correlation compares the current and previous images, rather than comparing the current image to the original undeformed reference image. The axial (1,x) and transverse (2,y) strains, calculated based on the deformations using the DIC algorithms, are used with the recorded axial loads for each load step (image) in the analysis methods described previously in Eq. 12 to generate the shear stress–strain plots for the materials (Fig. 8).

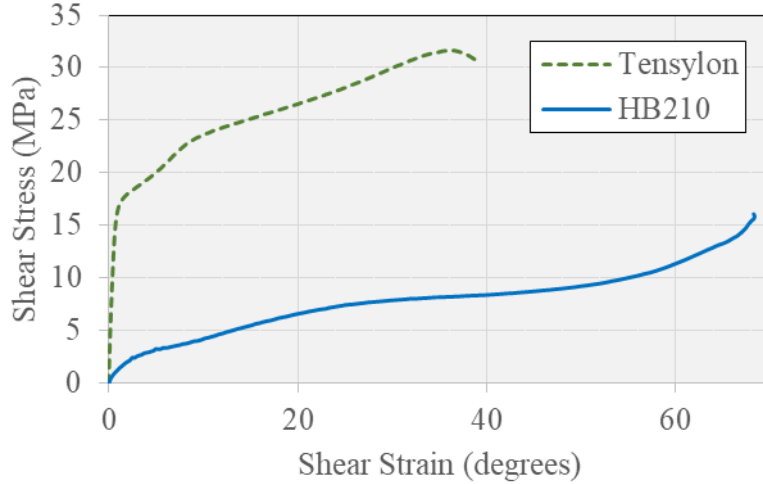


Fig. 8 Shear stress–strain response for fiber-based (HB210) and film-based (Tensylon) systems

Analysis of the DIC data (based on the method from Cline et al.⁵) indicates that all deformation is due to fiber rotation, thereby confirming the assumption that fiber elongation is negligible. Within the pure-shear region, the shear strain is confirmed uniform via DIC, indicating that the stress field is also uniform (and pure shear). The shear responses for both UHMWPE material systems, as calculated from Eq. 12, are shown in Fig. 8. There is significant shear deformation observed in the HB210 material system prior to failure, with the fibers rotating over 30°. The Tensylon 30A sheets are found to be significantly stiffer than the fiber-based system, but still undergo significant shear deformation prior to failure. The initial shear stiffness trend (shear stiffness values at lower shear angles) was previously reported by White et al.⁹ The reason for the stiffness difference is theorized to be that fibers embedded in a matrix material can slide relative to each other, which allows the UHMWPE to rotate much easier than in solid-state extruded film form.

3.2 Bias-Extension Simulation

A trilinear shear modulus curve is used as input to the numerical models of the bias-extension and picture frame simulations. The fit of this model to the in-plane shear response of HB210 from the bias-extension test is shown in Fig. 9. The trilinear model has small deviations from the test data at low shear angles (<7°) and those outside the range of interest (best fit curve was only up to 55°).

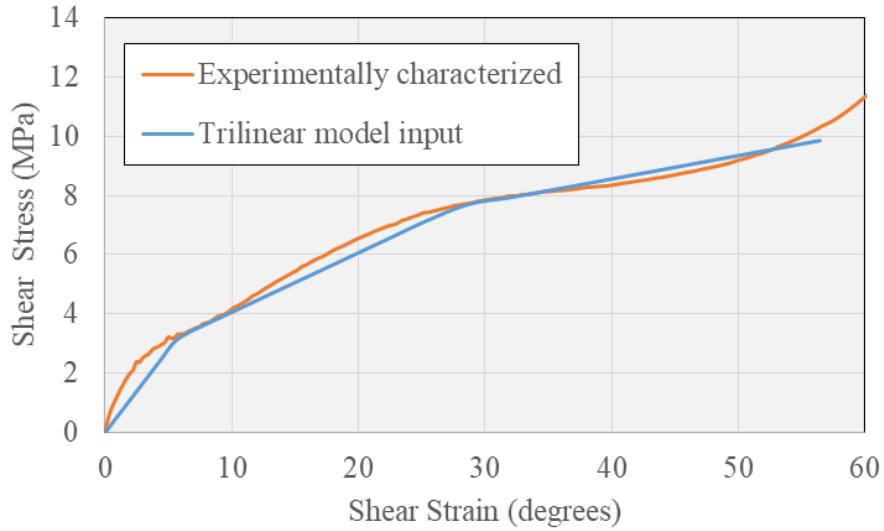


Fig. 9 Experimentally derived shear response and corresponding trilinear fit for HB210

The computational model allows for the prediction of shear strain at any location in a bias-extension specimen for each time step. The end boundary condition assumes no fiber rotation, resulting in negligible shear deformation along the top and bottom edges. The central region is in pure shear, while the ends have a shear strain gradient, shown in Fig. 10. There is only small deformation in the areas where there is a continuous fiber path to the top and bottom boundaries.

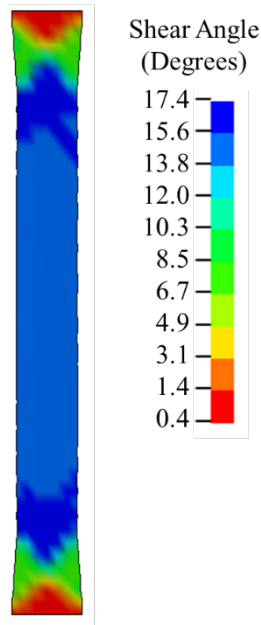


Fig. 10 Representative shear strain prediction for HB210 after 20 mm of crosshead displacement

The bias-extension numerical and experimental results for the UHMWPE fiber- and film-based systems are compared in Fig. 11. The axial strain measurements of the numerical model were taken from the pure shear region to ensure consistency with the DIC axial strain measurements. The DIC strain values are preferred over crosshead displacement because DIC does not include sources of error such as slippage and fiber rotation in the grips. The quality of agreement between the model and experimental results provides initial validation for the in-plane shear characterization and numerical model.

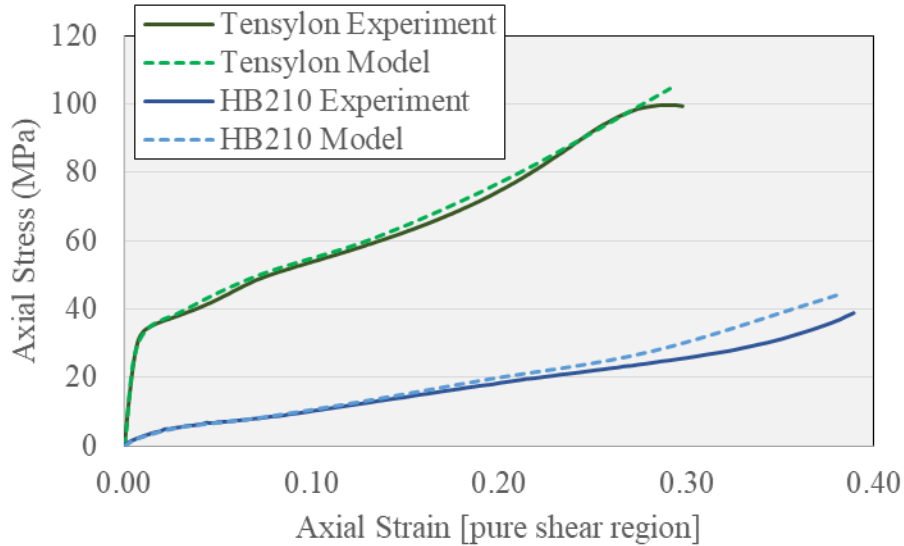


Fig. 11 Bias-extension simulation and experimental results for fiber-based (HB210) and film-based (Tensylon) systems

3.3 Picture Frame Model Predictions and Experimental Results

Full validation of both the bias-extension characterization methodology and corresponding model requires successful prediction of another test, such as the picture frame test, using the characterized bias-extension response as the input. Although the picture frame test faces significant challenges for film-based systems, it has been successful for fiber-based systems.⁹ The picture frame test, performed with HB210, provides a different loading pattern to evaluate the model performance with the DIC-based characterized shear properties.

The model successfully predicted the experimental results for crosshead load versus displacement curve, as shown in Fig. 12. Validation of the characterization and modeling techniques for the fiber-based system extends to the film-based system because the key assumption (all deformation modes other than shear deformation are negligible) made for the HB210 (fiber-based) is also valid for Tensylon (film-based).

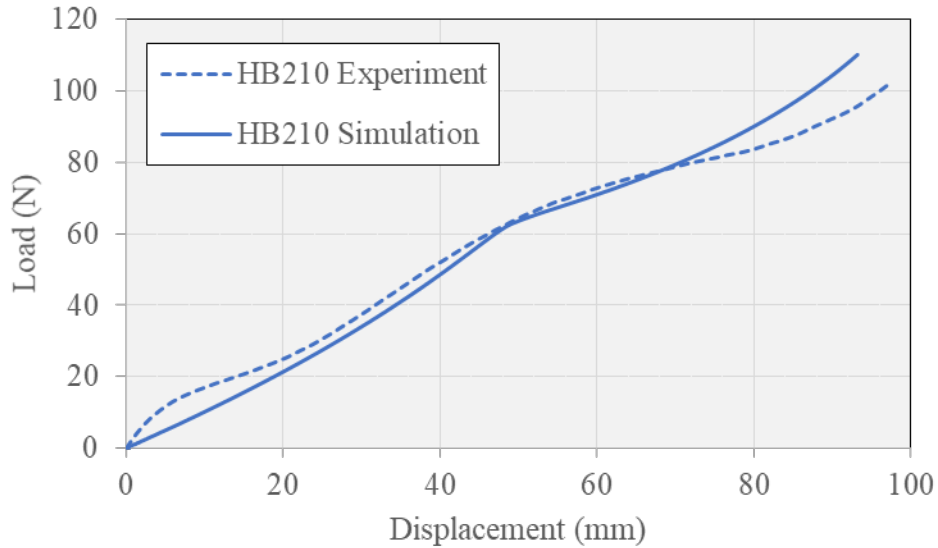


Fig. 12 Picture frame test simulation results, using characterized in-plane shear response, compared to experimental results

There were small deviations for the initial small displacements and toward the end of the test. These deviations are because the trilinear fit allowed some differences from the test data at the low- and high-shear angles, which was shown in Fig. 9. Increasing the number of line segments describing the shear stress–strain response would reduce these small deviations. However, increased accuracy at low displacement values would not add value to the overall body of work because the thickness changes induced by small in-plane shear values are negligible. The range of shear angles over which the curve was fit could be increased if increased accuracy at higher shear angles was desired, but that would not be relevant for this work because the range selected corresponds to the shear deformation found in hemisphere forming.¹

The picture frame test generally assumes a pure shear distribution in the central region of the specimens.⁸ The model predicted an almost pure shear region developing in the gage (central) area of the specimen, with small deviations along the boundary as shown in Fig. 13. There are also variations in the arms of the specimen, but these did not appear to significantly influence results. Notably, wrinkles developed vertically during the simulation, which was also evident in experimental results for UHMWPE systems.⁸

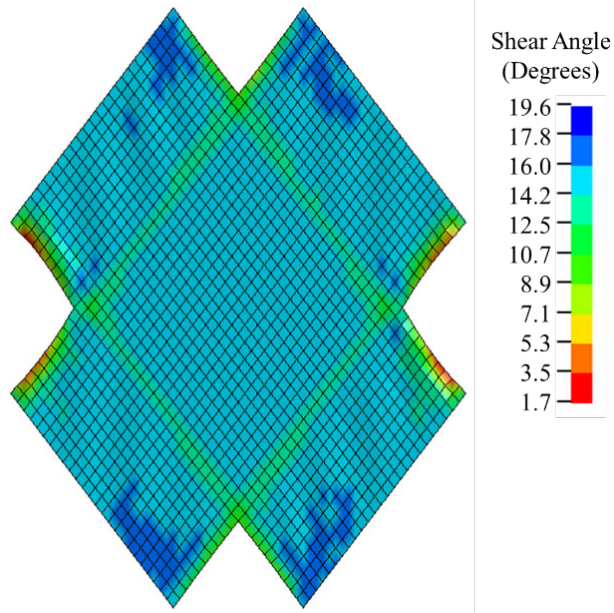


Fig. 13 Shear strain distribution in the picture frame model for HB210 at 40-mm crosshead displacement

4. Conclusions

The in-plane shear response of materials is a critical element in modeling the forming process. This work develops and validates a new in-plane shear characterization method capable of characterizing UHMWPE materials undergoing large shear strains, far beyond the capability of the current ASTM standard test method.¹³ The method is based on a simple tension test of laminates with a $[\pm 45^\circ]_2$ layup and uses DIC-based methods to measure the fiber rotation angles (shear strain) as a function of applied load. The shear strain measurements are coupled with a derived analytical calculation of the shear stress in the pure shear region to characterize the shear stress–shear strain constitutive response. This method is applied to UHMWPE fiber-based (Dyneema HB210) and film-based (Tensylon 30A) material systems. The simplicity of the method eliminates the complex test setup and data reduction schemes associated with the picture frame test, while at the same time expanding the material classes capable of being characterized.

Using the generated in-plane shear material properties from the bias-extension test, the LS-DYNA finite-element model accurately predicted the picture frame test results, validating both the characterization and modeling of UHMWPE shear deformation. The in-plane shear stiffness is much higher for Tensylon (film-based system) than Dyneema HB210 (fiber-based system). The fiber-based system has a higher failure shear strain, which is anticipated to allow it to deform much more during processing before damage is induced. This testing methodology will be used

to characterize materials' formability and provide inputs to a model of the manufacturing process.

5. References

1. Dangora LM, Mitchell C, Sherwood JA, Parker JC. Deep-drawing forming trials on a cross-ply thermoplastic lamina for helmet preform manufacture. *Journal of Manufacturing Science and Engineering*. 2017;139.
2. Cartwright B, Mulcahy NL, Chhor A, Thomas S, Suryanarayana M, Sandlin J, Crouch I, Maebe M. Thermoforming and structural analysis of combat helmets. *Journal of Manufacturing Science and Engineering*. 2015;137.
3. Dong L, Lekakou C, Bader MG. Sold mechanics finite element simulations of the draping of fabrics: a sensitivity analysis. *Composites Part A. Applied Science and Manufacturing*. 2000;31:639–652.
4. Zampaloni MA, Pourboghraat F, Yu W-R. Stamp thermo-hydroforming: a new method for processing fiber-reinforced thermoplastic composite sheets. *Journal of Thermoplastic Composite Materials*. 2016;17(1):31–50.
5. Cline J, Bogetti TA, Love B. Comparison of the in-plane shear behavior of UHMWPE fiber and highly oriented film composites. American Society for Composite Materials (ASC) 32nd Annual Technical Conference; 2017; West Lafayette, IN.
6. Bogetti TA, Walter M, Staniszewski J, Cline J. Interlaminar shear characterization of ultra-high molecular weight polyethylene (UHMWPE) composite laminates. *Composites Part A: Applied Science and Manufacturing*. 2017;98:105–115.
7. Lässig TR, May M, Heisserer U, Riedel W, Bagusat F, van der Werff H, Hiermaier SJ. Effect of consolidation pressure on the impact behavior of UHMWPE composites. *Composites Part B: Engineering*. 2018;147:47–55.
8. Dangora LM, Hansen CJ, Mitchell CJ, Sherwood JA, Parker JC. Challenges associated with shear characterization of a cross-ply thermoplastic lamina using picture frame tests. *Composites Part A: Applied Science and Manufacturing*. 2015;78:181–190.
9. White KD, Yeager M, Sherwood JA, Bogetti TA, Cline J. Material characterization and finite element modeling for the forming of highly oriented UHMWPE thin film and unidirectional cross-ply composites. American Society for Composites Technical Conference; 2018; Seattle, WA.

10. Cao J, Akkerman R, Boisse P, Chen J, Cheng HS, de Graaf EF, Gorczyca JL, Harrison P, Hivet G, Launay J et al. Characterization of mechanical behavior of woven fabrics: experimental methods and benchmark results. *Composites Part A: Applied Science and Manufacturing*. 2008;39:1037–1053.
11. Boisse P, Hamila N, Guzman-Maldonado E, Madeo A, Hivet G, dell'Isola F. The bias-extension test for the analysis of in-plane shear properties of textile composite reinforcements and prepregs: a review. *International Journal of Material Forming*. 2017;10(4):473–492.
12. Prodromou AG, Chen J. On the relationship between shear angle and wrinkling of textile composite preforms. *Composites Part A: Applied Science and Manufacturing*. 1997;28(5):491–503.
13. ASTM D3518/D3518M – 13. Standard test method for in-plane shear response of polymer matrix composite materials by tensile test of a $\pm 45^\circ$ laminate. West Conshohocken (PA): ASTM International; 2018.
14. Dyneema HB210. Hard ballistic solutions (insert, helmet, shield). [accessed 2019 Sep 5]. Heerlen (Netherlands): DSM. https://www.dsm.com/content/dam/dsm/dyneema/en_GB/Downloads/LP%20Product%20Grades/DSM_Hard_Ballistic_solutions.pdf.
15. Tensylon HSB30A bidirectional laminate. Midlands (MI): DuPont; c2013 [accessed 2019 Sep 5]. http://www.dupont.com/content/dam/dupont/products-and-services/personal-protective-equipment/vehicle-armor/documents/DPP_Tensylon30A_datasheet_K25929_2.pdf.
16. Rajan SD, Mobasher B, Vaidya A, Zhu D, Fein J, Deivanayagam A. Explicit finite element modeling of multilayer composite fabric for gas turbine engine containment systems, phase IV. Atlantic City (NJ): Federal Aviation Administration, Office of Aviation Research; 2014. Report No.: DOT/FAA/TC-13/37.
17. LS-DYNA user's manual, R10.0. Livermore (CA): Livermore Software Technology Corporation; 2017.

1 DEFENSE TECHNICAL
(PDF) INFORMATION CTR
DTIC OCA

1 CCDC ARL
(PDF) FCDD RLD CL
TECH LIB

1 GOVT PRINTG OFC
(PDF) A MALHOTRA

11 CCDC ARL
(PDF) FCDD RLW MA
BOGETTI TA
BOYD SE
CAIN J
STANISZEWSKI JM
TZENG J
WETZEL E
YEAGER M
FCDD RLW MB
CLINE JE
GRAY D
O'BRIEN D
WALTER T